Synchrotron-induced surface-photovoltage saturation at intercalated Na/WSe_2 interfaces

A. Schellenberger, R. Schlaf, C. Pettenkofer, and W. Jaegermann
Hahn-Meitner-Institut, Abteilung Solare Energetik, Glienicker Strasse 100, 1000 Berlin 39, Germany
(Received 15 July 1991)

The interaction of ultrahigh-vacuum cleaved *p*-type WSe_2 (0001) (band gap $E_G = 1.2$ eV) with deposited Na has been investigated by photoelectron spectroscopy using synchrotron radiation and low-energy electron diffraction. At room temperature (RT) the deposited Na diffuses into the bulk of the substrate (intercalation) and creates a compensated degenerate *n*-doped WSe_2 surface layer. At low temperatures (LT, 150 K) the deposited Na forms a metallic overlayer. For this condition a maximum surface photovoltage (SPV) of 0.8 eV is induced by synchrotron radiation. Annealing the sample at RT leads to a reduction of SPV and to intercalation of Na. After recooling the sample to LT the synchrotron-induced SPV is saturated (≈ 1 eV). The experimental values of the SPV for the different degrees of intercalation and temperatures are compared with theoretical estimates based on the expected values of the reverse dark current of Schottky diodes and *p-n* homojunctions. These estimations indicate the detrimental influence of the reverse dark current for the magnitude of the SPV response.

INTRODUCTION

The microscopic details of semiconductor-metal-interface (Schottky-barrier) formation are frequently investigated by photoelectron spectroscopy (PES) preferentially, with synchrotron radiation. PES provides spectroscopic information on the interface morphology (e.g., reactive versus nonreactive interfaces) and, in addition, on the electric potential distribution across the barrier (e.g., band-bending values and barrier heights), which is directly derived from the energetic shifts of the semiconductor photoelectron distribution curve (EDC) as a function of metal deposition. It was generally assumed that an electronic equilibrium situation is analyzed that is not disturbed by the photoelectron excitation radiation. However, a number of recent results indicate that this is not always the case.[1-9] The photoemission light source may induce a considerable number of electron-hole pairs within the semiconductor, which are separated in the built-in electric field of the space-charge layer, reducing the apparent value of band bending. The reported investigations on the photovoltaic effect in PES have indicated its strong dependence on sample temperature, semiconductor doping level, semiconductor band gap, and its rather weak dependence on light intensity.[1-10]

The surface-photovoltage (SPV) effect induced by external bias light illumination has frequently been used to characterize semiconductor junctions (e.g., surface-photovoltage spectroscopy) (see Refs. 11-17 and references therein) also in combination with photoemission experiments.[18-20]

Such bias-light-induced rebending of energy bands at semiconductor junctions (surface photovoltage or photovoltaic effect) is a well-known phenomenon used in energy conversion and light-intensity measurements (see, e.g., Refs. 21-23). Its quantitative dependence on semiconductor bulk and interface properties is important for the optimization of light-energy conversion efficiencies.

Especially, electronic surface and interface states may strongly influence the photovoltaic response of semiconductor junctions as they function as efficient recombination centers. For this reason it is favorable to investigate semiconductor interfaces which are chemically inert and free of surface states. The layered semiconductors such as WSe_2 are considered to be ideal substrates to study fundamental aspects of metal-semiconductor interaction. Their crystal structure is characterized by two-dimensional sheets of covalently bound *X-M-X* sandwiches which are separated from each other by only weak bonding interactions (van der Waals gap). The crystals can easily be cleaved across this gap; the resulting van der Waals plane (0001) contains a close-packed hexagonal array of chemically saturated chalcogenide ions. The ideal surface is considered to be free of surface states.[24] For this reason several investigations have been performed with respect to Schottky-barrier formation (see, for example, Refs. 20,25-29).

The layered compounds are known to insert alkali-metal and other small atoms into the van der Waals gap (intercalation).[30-32] The alkali-metal intercalation reaction is described by the rigid-band model.[33] The substrate lattice remains undisturbed within the *X-M-X* sandwich layer; therefore the electronic band structure is retained. As has been shown recently, ultrahigh-vacuum (UHV)-deposited alkali-metal atoms may be intercalated in *n*-type WS_2 and *p*-type WSe_2 (Refs. 34 and 35) with electron transfer from the alkali-metal to the conduction band of the host. As a consequence a compensated degenerate n^+-type doped material is formed.[34,35] The intercalation process is temperature-dependent,[35] which allows the transformation of the type of junction with temperature.

In this paper we present results of low-temperature (LT, 150 K) Na deposition on *p*-type WSe_2, the transformation of the junction (intercalation) with temperature, and the resulting junction properties. The room-

temperature (RT) deposition results have already been published in part elsewhere[35] and will be presented for comparison. The main emphasis of this study is to quantify the nonequilibrium response due to illumination (SPV). We are able to investigate the SPV response with one single crystal covered with Na which changes from a semiconductor-metal junction (p-type WSe_2/Na) to a p-n^+ homojunction in dependence on sample temperature. The clean surface and the adsorbate-induced changes were mainly investigated by photoelectron spectroscopy using synchrotron radiation of the BESSY storage ring. The results obtained for this specific semiconductor-metal interface may be related to other semiconductor-metals barriers, in which interdiffusion of the adsorbed metals cannot be excluded entirely.

EXPERIMENT

Single crystals of p-type WSe_2 were prepared by sublimation with excess Se in sealed quartz tubes which leads to p-doped material (doping density 10^{17} cm^{-3}).[36] Typical dimensions of the crystals were $5\times5\times0.1$ mm^3. The crystals were attached to a Cu sample holder by Ag epoxy and cleaved in UHV. Perfectly clean, mirrorlike (0001) surfaces can be obtained by this procedure. The cleavage plane shows a bright (1×1) hexagonal low-energy-electron-diffraction (LEED) pattern on a very low diffuse background as expected for the (0001) plane. Perfectly cleaved semiconductor samples do not show any band bending (flatband conditions) as deduced from the position of the valence-band maximum with respect to E_F (determined by the Cu sample holder or a Au reference). In addition, they show only small spectral shifts with decreasing sample temperature (<0.05 eV). The given temperatures were determined by a thermocouple in contact to the sample holder. Na was deposited from SAES getter sources with typical currents of 7.5 A at room temperature (RT) and 7 A at low temperature (LT). From a consideration of producer-supplied information and the geometric conditions of the Na source, exposure time of about 10 s at 7.5 A corresponds to one monolayer equivalent dose. For RT conditions a Na-to-WSe_2 intensity ratio of 1 is obtained after 9-min deposition time (considering theoretical cross sections[37]).

The photoemission experiments were performed in an angle-resolving electron spectrometer (VG ADES 500, normal emission). The base pressure of the UHV system was below 1×10^{-10} mbar. No oxidation of the deposited Na was detected during the experiments. As excitation source synchrotron light [BESSY storage ring, TGM 7, $h\nu=80$ eV (Ref. 38)] was used. The photoelectron spectra were calibrated versus the Fermi edge of metallic samples (Cu, Au) which were cleaned by Ar-ion etching before cleaving the crystals. A negative bias voltage of 6 V was applied to the sample to ensure a reliable determination of the sample work function.

RESULTS

The photoemission spectra of the cleaved surfaces show sharp W $4f$ emission lines [full width at half maximum (FWHM)$=0.3$ eV] and slightly broader Se $3d$ lines (FWHM$=0.39$ eV). The valence-band spectra show the onset of photoemission (valence-band maximum E_{VB}) at 0.1 eV below the Fermi level E_F, which is consistent with the doping of the sample and flatband conditions after cleavage. The work function ϕ for different samples is determined from the secondary electron onset as 5.2 ± 0.3 eV.

During RT deposition the WSe_2 core levels (Fig. 1) and valence-band features remain unchanged with increasing Na deposition compared to the clean surfaces. We do not detect any sign of an exchange reaction of Na with the substrate which would lead to chemical shifts of the core-level emission lines. The Na $2p$ emission (Fig. 1) grows in as a broad line (FWHM$=1.2$ eV) which is identical to the spectra obtained for Na inserted into SnS_2.[35]

The changes of surface potentials (shift of the binding energy ΔE_B and work-function change $\Delta\phi$) in the course of Na deposition at RT are summarized in Fig. 2. The substrate binding energies are increased with increasing Na coverage, which indicates a movement of the Fermi level from a position close to the valence band towards the conduction band. The saturation value of ΔE_B of 0.85 eV has to be related to the band gap of 1.2 eV (Ref. 39) and the distance E_F-E_{VB} of 0.1 eV. We did not observe the formation of a clear Fermi edge for these conditions; for this reason we could not determine whether any SPV is induced by the probing light. It is possible to induce a SPV of 0.2 eV reducing ΔE_F by illuminating the sample with white bias light (W/halogen lamp, 100 mW/cm^2). As the maximum SPV value can be estimated to be below 0.25 eV, which is the difference $E_G-\Delta E_B-(E_F-E_{VB})$, we may conclude that no SPV is generated by the synchrotron light.

The work function ϕ is continuously reduced as a function of Na dose; after 6-min gradual deposition [I(Na-W)$=13\%$ considering theoretical cross sections[37]] it is

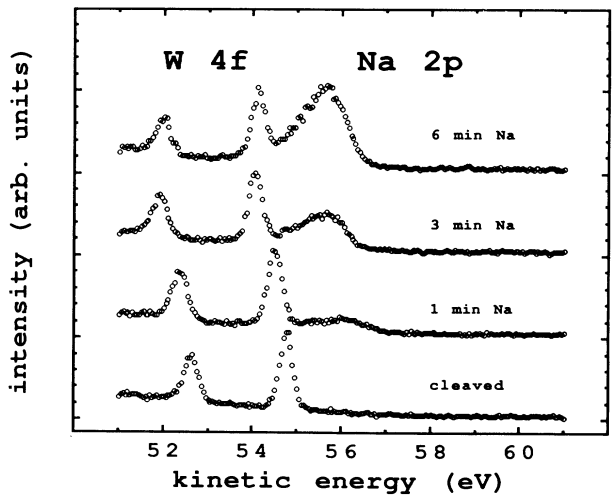

FIG. 1. Photoemission lines of the W $4f$ and Na $2p$ core levels during Na deposition on WSe_2 at RT. The spectra were taken with synchroton light (photon energy $h\nu=80$ eV) and given in kinetic energy (a negative bias voltage of 6 eV was applied).

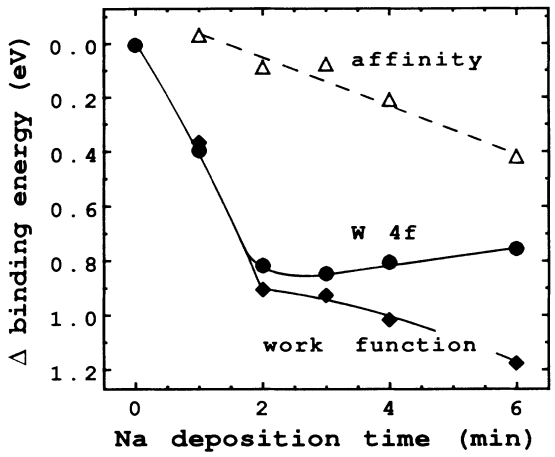

FIG. 2. Changes of surface potentials in the course of Na deposition at RT. The binding-energy shift ΔE_B is deduced from the W $4f$ core levels; the work-function change $\Delta\phi$ is given by the shift of the secondary-electron onset. The electron affinity is calculated as $\Delta\phi - \Delta E_B$.

decreased by 1.2 eV to a final value of about 4 eV. This value is composed of a Fermi-level shift ΔE_B of 0.85 eV and an additional contribution of an electron affinity change of 0.35 eV due to the Na-induced surface dipole change. It is considerably different from the value reported for metallic Na ($\phi_{Na}=2.75$ eV).[40,41]

We performed LEED experiments after different amounts of deposited Na in a subsequent experiment. A change in the hexagonal LEED pattern of the (0001) surface was not observed; only the diffuse background was slightly raised. Evidently the structure of the X-M-X sandwich layer remains unaffected. A sodium-induced superstructure was not formed for our experimental conditions up until dosages exceeding 9 min.

In Fig. 3 we present the photoemission spectra of the W $4f$ and Na $2p$ levels in the course of Na deposition at low temperatures (150 K). First only the changes of spectral features will be discussed. The energy shifts due to changes of surface potentials (ΔE_B, $\Delta\phi$, and SPV) will be considered later. The Na $2p$ levels show for small coverages only a very weak and rather broad emission feature. In contrast to the RT results, a sharp emission line of Na grows in for higher deposition times (>6-min FWHM=0.5 eV), which is related to the formation of a metallic Na overlayer. It is known from alkali-metal deposition on different substrates that sharp emission lines of the alkali-metal overlayer are obtained for metallic multilayers.[42–44] The attenuation of the substrate emissions indicates that the overlayer grows in the form of clusters. When the sample temperature is raised to 300 K, the intercalation of the metallic Na overlayer into the substrate sets in and is completed within 8 h. This is deduced from the transformation of the Na $2p$ levels to a broad emission peak shifted to higher binding energies (Fig. 3), which corresponds to the room-temperature deposition results (Fig. 1). The substrate emission lines are not significantly affected. Only the FWHM is increased by about 200 meV for the W $4f$ and the Se $3d$ lines during all experimental sequences described above. For the transformed interface the stoichiometry is estimated from the intensities as Na_xWSe_2 ($x\sim 0.1$).

In Fig. 4 the valence-band region of WSe_2/Na is shown for significant experimental conditions. Due to the formation of the metallic overlayer at LT the valence-band features decrease in intensity and change their shape. After annealing at RT and intercalation of the metallic Na overlayer the original WSe_2 spectrum is restored again (with a small change in the intensity pattern). A Fermi edge is clearly established in the LT valence-band spectra containing the metallic Na overlayer (see the inset in Fig. 4). For the intercalated Na/WSe_2 we were not able to determine a clearly developed Fermi edge.

The secondary-electron onset shows two different cutoffs. The lower one increases in intensity with increasing Na coverages at LT deposition and is therefore related to the contribution of the metallic Na deposits. The corresponding work function ϕ is determined as 3.5 eV. When the shift of E_F due to the SPV (0.8 eV, see later) is subtracted this number is close to the reported value of

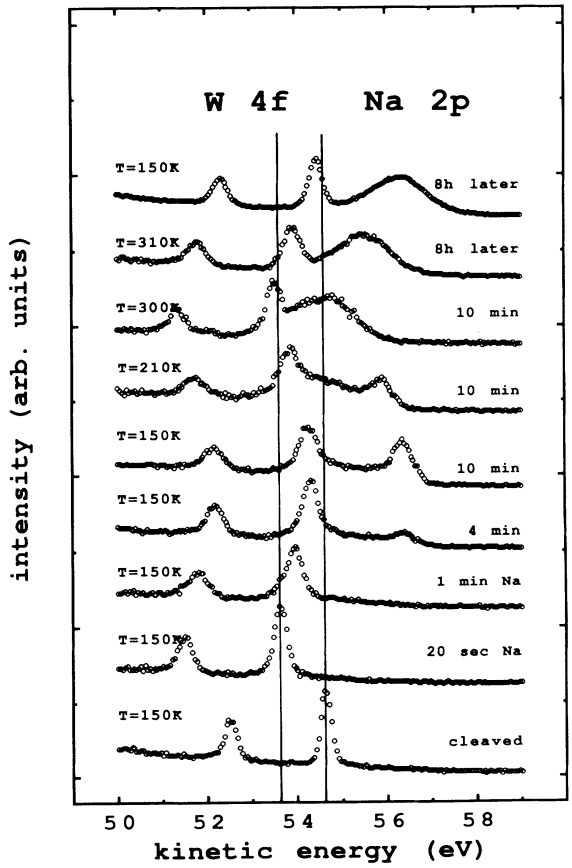

FIG. 3. Synchrotron-induced photoemission spectra for the W $4f$ and Na $2p$ levels in the course of Na deposition at low temperatures LT (150 K) and during annealing. The spectra are taken with a photon energy of $h\nu=80$ eV and given in kinetic energy (a negative bias voltage of 6 eV was applied to the sample).

metallic Na ($\phi_{Na}=2.75$ eV).[40,41] During RT annealing ϕ increases to 3.8 eV which agree reasonably with the value obtained in the RT deposition experiments.

By RT annealing the Na/WSe_2 metal-semiconductor interface is transformed to the same intercalation layer that is readily formed at RT deposition. We will now consider the shift of the Fermi level during LT deposition and subsequent RT annealing and recooling in more detail. The LT alkali-metal-induced binding-energy shifts are plotted in Fig. 5(a) in the course of Na deposition. After an initial strong Fermi-level shift for small Na coverages, which corresponds to a downward bending of energy bands as expected for p-type WSe_2/Na interfaces, the energy position for higher Na coverages shifts back towards the initial position observed for the clean surface. For these conditions the Fermi edge of the Na overlayer is found 0.8 eV above the Fermi edge of the metallic Cu sample holder (reference level; see the inset in Fig. 4). We also include the movement of the Fermi edge of the Na overlayer into Fig. 5(a). This negative shift of the Fermi edge binding energy from its reference level ($E_B=E_F=0$ eV) is related to the buildup of the SPV response induced by the synchrotron radiation. It is evident from this plot that also the reverse shift of the substrate core-level emission lines is due to the SPV. Its magnitude is considerably larger compared to the values observed by other authors,[1-9] especially when the low band gap of WSe_2 of 1.2 eV and moderately low sample temperatures are considered.

By increasing the sample temperature the SPV is gradually reduced, shifting the EDC back to the expected value for strong band bending [Fig. 5(b)]. Simultaneously the interface is transformed due to the intercalation of the metallic Na deposits. As a consequence the WSe_2/Na Schottky barrier is transformed to a diffused WSe_2 p-n^+ homojunction. At this stage an additional SPV of 0.25

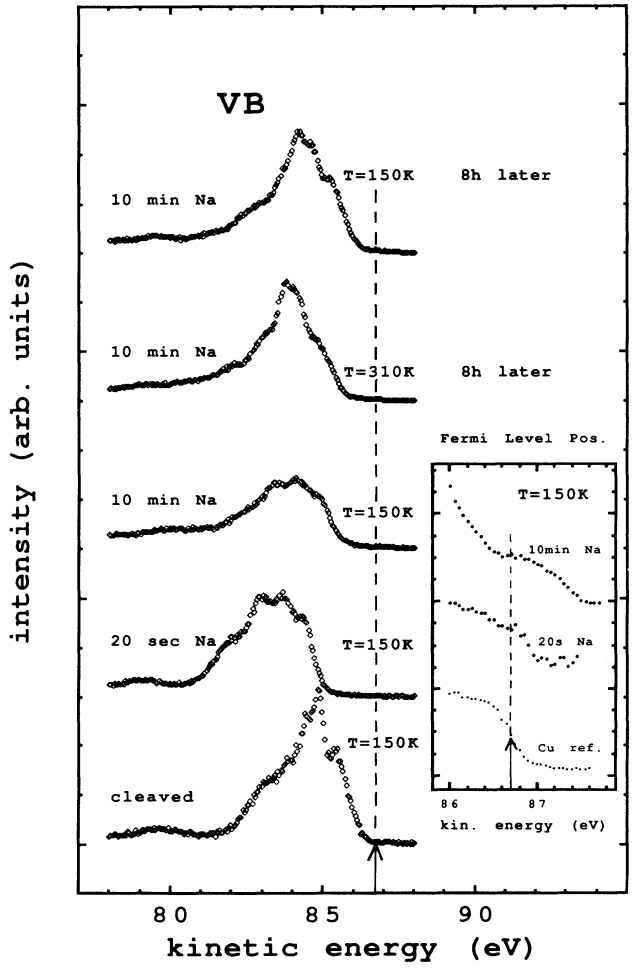

FIG. 4. Valence-band spectra of WSe_2/Na shown for specific and significant experimental conditions of the interface as defined in Fig. 3. Changes in Fermi-level position by generating a surface photovoltage are shown in the inset (the arrow indicates the Fermi-level position for the copper sample holder). The upper two curves show the photoemission spectra after annealing at room temperature and after recooling. The spectra are taken with a photon energy of $h\nu=80$ eV and are given in kinetic energy (a negative bias voltage of 6 eV was applied).

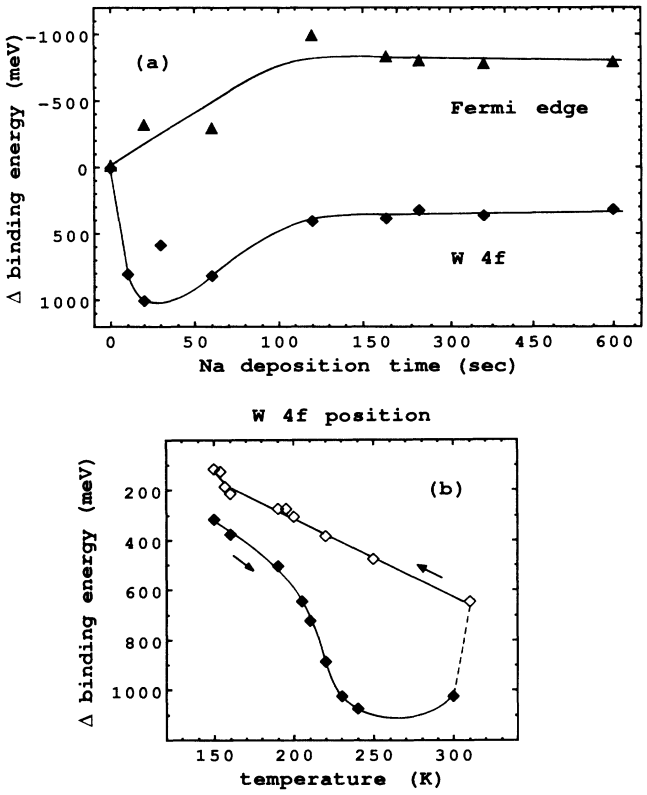

FIG. 5. (a) The alkali-metal-induced binding-energy shift of W 4f and the SPV derived from the shift of surface Fermi-edge position plotted against the Na deposition time ($T=150$ K). At 10-min deposition time the Fermi edge of the Na overlayer is found 0.8 eV above the Fermi edge of the metallic sample holder $E_F=0$ eV (reference level; see also the inset of Fig. 4). (b) Temperature-dependent binding-energy shift of W 4f of p-type WSe_2/Na (10-min deposition) plotted vs temperature T during annealing to 310 K (filled squares) and during recooling down to 150 K (open squares).

eV can be induced by an external white light source of high power (100 mW/cm^2).

After annealing the sample overnight (8 h) the synchrotron-light-induced SPV is at least 0.5 eV at RT. When the sample temperature is decreased again to 150 K the spectral features do not change any more. But we observe a SPV induced by the synchrotron light which is even larger as obtained before the room-temperature surface transformation occurred [Fig. 5(b)]. We approach for the core-level emission lines the binding-energy position before starting the alkali-metal deposition. Evidently it is possible to saturate the SPV under these conditions, completely rebending the energy bands (SPV ≥ 1 eV). As the experimental conditions were identical in all experiments (besides the reported temperature variations) the strongly affected SPV response is evidently due to considerably changed junction properties.

DISCUSSION

Electronic structure of the intercalated $Na_x WSe_2$

The electronic structure of transition-metal dichalcogenides intercalation compounds have been discussed in many review articles and books (see e.g., Refs. 30–33 and 45). However, only very few self-consistent band-structure calculations have been published so far: on $LiTiS_2$ (Refs. 46 and 47) and $MTaS_2$ (M=Sn,Pb,Ge).[48] In addition, most of the intercalation studies have been directed to the group-IV B and -V B dichalcogenides and only a very limited number of physical studies have been reported for group-VI B dichalcogenides as for its prototype compound MoS_2 or WSe_2.[49] In a first and reasonable approximation the intercalation process of, e.g., alkali-metal can be described for most transition-metal dichalcogenides in terms of the rigid-band model (see, e.g., Refs. 32 and 33). The structure of the two-dimensional X-M-X sandwiches remains mainly undisturbed by intercalation. In dependence on its size the alkali-metal ion occupies the octahedral or trigonal prismatic coordination sites in the van der Waals gap. The s electron of the alkali-metal is nearly completely transferred into the unchanged empty electron bands of the dichalcogenide host material: the inserted alkali-metal is oxidized and the metal dichalcogenide layer is reduced. The electronic properties of the resulting intercalation phase is thus dependent on the electronic band structure of the host material for which a large number of calculations exists (see, e.g., Refs. 50 and 51).

There is no evidence for any structural changes of the Na intercalated WSe_2 as is derived from our LEED results and the photoelectron spectra. Therefore we would like to interpret our photoelectron spectra obtained from the Na-intercalated WSe_2 based on the rigid-band model. In Fig. 6 we show the density-of-state (DOS) distribution of $MoSe_2$, which was obtained by self-consistent band-structure calculations.[52] In addition, we show a schematic DOS (Ref. 33) with the main atomic orbital contribution of the respective band and the number of available electron states per formula unit. The valence-band maximum in WSe_2 is derived from the W $5d_{z^2}$ level. For this semiconducting compound the d_{z^2} level is completely filled with electrons. It is only half filled for the more often studied metallic group-V B dichalcogenides. The Fermi level is situated 0.1 eV above the valence-band maximum for the p-doped sample. After intercalation of the deposited Na the conduction band, which is mainly derived by the W $5d_{xy,x^2-y^2}$ levels will be partly filled by the electrons from the alkali metal. Based on the deter-

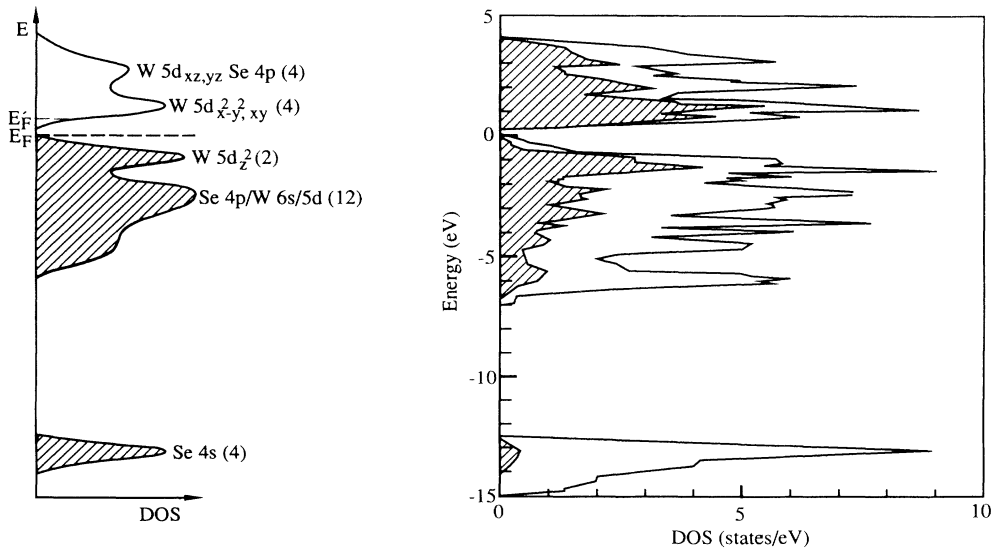

FIG. 6. Schematic density of states (left) for WSe_2 (occupied states are hatched) and Fermi-level position before (E_F) and after intercalation (E_F'). For comparison the calculated density of states for the isoelectronic $MoSe_2$ (Ref. 52) is shown on the right. Depicted is the total and partial (hatched) Mo-derived density of states.

mined Na stoichiometry (Na_xWSe_2, $x \approx 0.1$) we expect an occupation of this band with about 0.1 electron per formula unit, which is 1/40 of its capacity. This number translates to an approximate electron density of 10^{21} electrons/cm^3, which transforms the intercalated surface phase to a strongly degenerate n^+- type semiconductor or semimetal. The Fermi level is situated within the original conduction band (Fig. 6). As a consequence the alkali-metal-intercalated group-VI B dichalcogenides should show increased (metallic) conductivity, which has been proven experimentally.[49]

Barrier properties

In this subsection we would like to discuss the consequences of Na intercalation for the optoelectronic junction properties. At low temperatures (150 K) it is evidently possible to freeze the in-diffusion of the Na atoms. A metallic overlayer is formed (Fig. 7, left); we deal with a Schottky barrier. At RT the alkali metal is intercalated and a degenerate n-type doped surface layer is formed; the barrier resembles a p-n^+ homojunction (Fig. 7, right).

It is not possible to discriminate strong band bending and the redoping of the surface layer from the shifts of the photoemission spectra in the RT results (Fig. 1). For p-type semiconductors strong downward bending of energy bands as well as compensation doping to n type will lead to comparable shifts of the Fermi level with respect to the valence-band maximum.

However, the LT results clearly indicate the differences in junction properties, especially when the magnitude of the SPV is evaluated. In order to evaluate the synchrotron-induced SPV for the two different kinds of junctions, a simple estimate is performed.

For idealized solid-state junctions the open circuit photovoltage U_{ph} corresponding to the SPV is given by[21–23]

$$U_{ph}=(kT/e)\ln(i_{ph}/i_0+1) .$$

In a simple model the photocurrent density i_{ph} is determined by the incident photon density I_0, the bias-dependent width of the space-charge layer W, the light absorption constant α, and the diffusion length L_d of the minority carriers in the field-free region (Gärtner model)[53]

$$i_{ph}=I_0\left[1-\frac{\exp(-\alpha W)}{\alpha L_d}\right] .$$

In our case W is approximately 1000 Å, α is in the range of 10^5 cm^{-1}, and L_d is about 1 nm,[54] therefore the photocurrent is directly given by I_0.

The number of incident photons I_0 due to the synchrotron light was estimated from the measured photoelectric yield current on a gold film as 4×10^{11} photons/s. The light spot on the sample was determined to be about 0.3×1.5 mm. Assuming a quantum efficiency of $E_{h\nu}/3E_G=22$ (Ref. 55) for electron-hole-pair generation per photon (using synchrotron light of $h\nu=80$ eV) and negligible bulk recombination we get 2×10^{15} electrons/s^1 cm^2, which corresponds to the photocurrent of $i_{ph}=3\times10^{-4}$ A/cm^2.

For steady-state condition at open circuit the majority carrier dark current i_d counteracts the electron-hole separation in the electric space-charge layer, which is responsible for the photovoltage effect. Its magnitude is dependent on the mechanism of charge injection from the semiconductor to the contact phase. For ideal semiconductor-metal interfaces this reverse current is determined by the thermionic emission of the charge carriers over the barrier (neglecting the smaller contributions of field emission through the barrier for doping levels below 10^{17} cm^{-3}):[21]

$$i_0=A^*T^2\exp(-q\Phi_B/kT)$$

($A^*=4\pi qm^*k^2h^{-3}$ is a modified Richardson constant; Φ_B is the experimentally determined Schottky-barrier height). For p-n^+ homojunctions formed by intercalation, the dark current is given by the diffusion model[21] as

$$i_0=qD_pp_{n_0}/L_p+qD_nn_{p_0}/L_n$$

[$D_p=q^{-1}kT\mu_h$ is the diffusion constant (Einstein relation), μ_h is the hole mobility, $p_{n_0}=(N_CN_V/N_D)\exp(-E_G/kT)$ is the minority carrier concentration (no voltage applied), N_C,N_V are the effective densities of

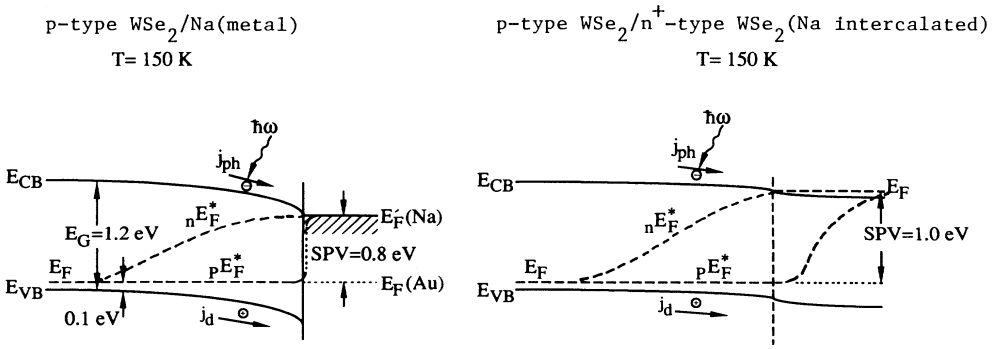

FIG. 7. Schematic picture of the junction formed by exposure to Na for different preparation conditions. Left: Schottky barrier; right: p-n homojunction after indiffusion of Na. The junctions are shown for nonequilibrium conditions at low temperatures.

states at the band edges, L_p is the diffusion length, and in analogy for the n-type doped side of the semiconductor, other symbols were used in the usual meanings].

In Fig. 8 the calculated and experimental values of U_{ph} for Schottky diodes and p-n^+ homojunctions are plotted against the temperature T, using $\mu_h = 236\ cm^2 V^{-1} s^{-1}$, $\mu_e = 105\ cm^2 V^{-1} s^{-1}$, $N_C = N_V = 1 \times 10^{19}\ cm^{-3}$,[36] $L_p = 0.1\ \mu m$ (value for low-Ohmic p-type WSe_2), and $L_n = 0.6\ \mu m$ (averaged value for high-Ohmic n-type WSe_2).[55] In addition, the temperature dependence of the band gap is taken into account and a linear dependence with the slope $dE_G/dT = 0.46$ meV is assumed.[56] E_G can now be written as

$$E_G = (1.36 - 4.6 \times 10^{-4} T)\ \text{eV} .$$

The important parameter for the maximum and minimum curves of U_{ph} is the effective mass of holes m^* in the case of Schottky diode behavior and $N_C N_V / N_D$ in the case of p-n homojunction behavior, as precise values for these quantities are not known.

It should be noted that the assumption of ideal solid-state junctions may be questionable. Deviations from ideal junction properties such as, e.g., space-charge recombination and/or field-assisted tunneling processes due to band-gap states, would increase i_0 and thus decrease U_{ph} (e.g., Ref. 21). On the other hand, the model is based on charge-carrier recombination velocities close to infinity within the metal overlayer, which might not be the case for metal clusters noncontinuously covering the surface. Slower recombination rates would increase the surface photovoltage.[21]

The theoretical estimate of the SPV effect indicates that the thermionic emission model of the Schottky junction reasonably describes the results of the nonintercalated junction. After annealing at RT and intercalation, the diffusion model of a p-n homojunction holds. During recooling, the experimental values of U_{ph} are clearly above the experimental values before annealing the junction. At 150 K, $U_{ph} \approx 1.0$ eV, which is a value clearly above the maximum SPV expected for a Schottky junction.

The higher SPV response of the p-n homojunction due to the intercalated phase (compare Fig. 8) mainly results from lower reverse dark currents ($< 1/1000$) compared to semiconductor-metal junctions.[22,23] In addition, it should be noted that the theoretical estimates given an upper limit of expected SPV response. Real junctions exhibit additional temperature-dependent loss mechanisms (see Refs. 36 and 57) which would shift the theoretical curves closer to the experimentally determined SPV values.

SUMMARY AND CONCLUSIONS

In this paper we have presented experimental results showing that the intercalation of layered compounds can be investigated *in situ* by UHV techniques. The alkali-metal intercalation of WSe_2 follows the rigid-band model: the extra electron of the alkali metal is transferred to unoccupied electron states of the host material. As a consequence the p-type doped WSe_2 substrate is transformed to an n^+-type doped surface layer. At low temperatures the Na intercalation is frozen out and a Na overlayer is formed. Therefore we could investigate a semiconductor interface, which changes its character as a function of temperature. In the center of our interest was the magnitude of the SPV effect for the different conditions of the interface. After intercalation the SPV induced by synchrotron radiation was strongly increased due to the transformation of the Schottky barrier to a p-n^+ homojunction. In conclusion, our results have demonstrated the importance of the junction properties, especially the dominant mechanism of charge injection for the surface photovoltage response. The most crucial parameter is the reverse dark current i_0 which may vary by many orders of magnitude for different injection processes.[21–23] For this reason a measurement of the SPV effect is a very sensitive tool to characterize the interface of semiconductor junctions also in UHV experiments. Such nonequilibrium measurements allow one to discriminate much more easily differences of junction properties as in the usually applied equilibrium measurements.

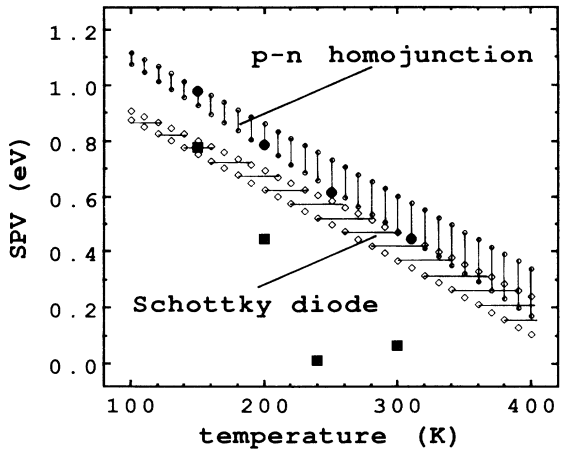

FIG. 8. Experimental values of the surface photovoltage (SPV) during annealing and recooling the junction p-type WSe_2/Na (10-min deposition) compared with theoretical curves estimated for Schottky diodes (open squares) and p-n^+ homojunctions (open circles). For details of the calculation see the text. The filled squares represent the SPV after deposition at 150 K and during annealing up to RT. After annealing at RT and during recooling the values of SPV are significantly increased (filled circles).

ACKNOWLEDGMENTS

We would like to thank Dr. M. Lux-Steiner for providing the crystals used in these experiments. We also would like to thank Dr. W. Braun and Dr. E. Holub-Krappe for their help in establishing the TGM-7 monochromator at BESSY. The friendly and continuous support of Professor H. Tributsch is also gratefully acknowledged. This work was supported by a grant of the Bundesminister für Forschung und Technologie.

[1]P. John, T. Miller, T. C. Hsieh, A. P. Shapiro, A. L. Wachs, and T. C. Chiang, Phys. Rev. B **34**, 6704 (1986).
[2]M. Alonso, R. Cimino, and K. Horn, Phys. Rev. Lett. **64**, 1947 (1990).
[3]C. M. Aldao, G. D. Waddill, P. J. Benning, C. Capasso, and J. H. Weaver, Phys. Rev. B **41**, 6092 (1990).
[4]M. Hecht, Phys. Rev. B **41**, 7918 (1990).
[5]K. Jacobi, U. Myler, and P. Althainz, Phys. Rev. B **41**, 10 721 (1990).
[6]S. Chang, I. M. Vitorimov, L. J. Brillson, D. F. Rioux, P. D. Kirchner, G. D. Pettit, J. M. Woodall, and M. H. Hecht, Phys. Rev. B **41**, 12 299 (1990).
[7]D. Mao, A. Khan, M. Marsi, and G. Margaritondo, Phys. Rev. B **42**, 3228 (1990).
[8]G. D. Waddill, T. Komeda, Y.-N. Yang, and J. H. Weaver, Phys. Rev. B **41**, 10 283 (1990).
[9]M. Alonso, R. Cimino, Ch. Maierhofer, T. Chassé, W. Braun, and K. Horn, J. Vac. Sci. Technol. B **8**, 955 (1990).
[10]J. E. Demuth, W. J. Thomson, N. J. DiNardo, and R. Imbihl, Phys. Rev. Lett. **56**, 1408 (1986).
[11]A. Many, Y. Goldstein, and N. B. Grover, *Semiconductor Surfaces* (North-Holland, Amsterdam, 1963).
[12]*Surface Physics of Phosphors and Semiconductors,* edited by C. E. Reed and C. G. Scott (Academic, London, 1975).
[13]H. C. Gatos and J. Lagowski, J. Vac. Sci. Technol. **10**, 130 (1973).
[14]H. Lüth and G. Heiland, Nuovo Cimento **39**, 748 (1977).
[15]J. Clabes and M. Henzler, Phys. Rev. B **21**, 625 (1980).
[16]L. J. Brillson and D. W. Krueger, Surf. Sci. **102**, 518 (1981).
[17]B. Adamowicz, Surf. Sci. **231**, 1 (1990).
[18]G. Margaritondo, L. J. Brillson, and N. G. Stoffel, Solid State Commun. **35**, 277 (1980).
[19]W. Jaegermann, Chem. Phys. Lett. **126**, 301 (1986); Ber. Bunsenges. Phys. Chem. **92**, 537 (1988).
[20]W. Jaegermann, C. Pettenkofer, and B. A. Parkinson, Phys. Rev. B **42**, 7487 (1990).
[21]S. M. Sze, *Physics of Semiconductor Devices* (Wiley, New York, 1981).
[22]H. J. Hovel, in *Solar Cells,* edited by R. R. Willardson and A. C. Beer, Semiconductor and Semimetals Vol. 11 (Academic, New York, 1975).
[23]A. L. Fahrenbruch and R. H. Bube, *Fundamentals of Solar Cells* (Academic, New York, 1983).
[24]E. Pehlke and W. Schattke, J. Phys. C **20**, 4437 (1987).
[25]W. Jaegermann, F. S. Ohuchi, and B. A. Parkinson, Surf. Sci. **194**, 269 (1988); Surf. Interf. Anal. **12**, 293 (1988); Surf. Sci. **201**, 211 (1988).
[26]G. J. Hughes, A. McKinley, R. M. Williams, and I. T. McGovern, J. Phys. C **15**, L159 (1982).
[27]I. T. McGovern, E. Dietz, H. H. Rothermund, A. M. Bradshaw, W. Braun, W. Radlik, and J. F. McGilp, Surf. Sci. **152/153**, 1203 (1985).
[28]J. L. Lince, D. J. Carre, and P. D. Fleischhauer, Phys. Rev. B **36**, 1647 (1987).
[29]T. Tambo and C. Tatsuyama, Surf. Sci. **222**, 332; 343 (1989).
[30]*Intercalation in Layered Materials, Nato Advanced Study Institute Series B: Physics,* edited by M. S. Dresselhaus (Plenum, New York, 1986), Vol. 148.
[31]*Intercalation Chemistry,* edited by M. S. Whittingham and A. J. Jacobson (Academic, New York, 1982).
[32]*Intercalated Layered Materials,* edited by F. A. Levy (Reidel, Dordrecht, 1977).
[33]W. Y. Liang, in Ref. 30, p. 31ff.
[34]F. S. Ohuchi, W. Jaegermann, C. Pettenkofer, and B. A. Parkinson, Langmuir **5**, 439 (1989).
[35]A. Schellenberger, R. Schlaf, T. Mayer, E. Holub-Krappe, C. Pettenkofer, W. Jaegermann, U. A. Ditzinger, and H. Neddermeyer, Surf. Sci. Lett. **241**, L25 (1991).
[36]R. Späh, Ph.D. thesis, University of Konstanz (1986); R. Späh, U. Elrod, M. Lux-Steiner, E. Bucher, and S. Wagner, Appl. Phys. Lett. **43**, 79 (1983).
[37]J. Yeh and I. Lindau, At. Data Nucl. Data Tables **32**, 1 (1985).
[38]E. Holub-Krappe *et al.*, BESSY Jahresbericht (1989) (unpublished).
[39]K. K. Kam, Ph.D thesis, Iowa State University (1982); K. K. Kam, C. L. Chang, and D. W. Lynch, J. Phys. C **17**, 4031 (1984).
[40]N. D. Lang and W. Kohn, Phys. Rev. B **3**, 1215 (1971).
[41]R. J. Whitefield and J. J. Brady, Phys. Rev. Lett. **26**, 380 (1971).
[42]P. Soukiassian, M. H. Bakshi, Z. Hurych, and T. M. Gentle, Surf. Sci. **221**, L759 (1989).
[43]M. Prietsch, M. Domke, C. Laubschat, T. Mandel, C. Xue, and G. Kaindl, Z. Phys. B **74**, 21 (1989).
[44]K. Horn, J. Somers, Th. Lindner, and A. M. Bradshaw, in *Physics and Chemistry of Alkali Metal Adsorption,* edited by H. P. Bonzel, A. M. Bradshaw, and G. Ertl (Elsevier, Amsterdam, 1989).
[45]R. H. Friend and A. D. Yoffe, Adv. Phys. **36**, 1 (1987).
[46]C. Umrigar, D. E. Ellis, D.-S. Wang, H. Krakauer, and M. Posternak, Phys. Rev. B **26**, 4935 (1982).
[47]F. V. McCanny, J. Phys. C **12**, 3263 (1979).
[48]F. Dijkstra, E. A. Broekhuizen, C. F. van Bruggen, C. Haas, R. A. de Groot, and H. P. van der Meulen, Phys. Rev. B **40**, 1214 (1989).
[49]S. B. Somoano and J. A. Woollam, in Ref. 32, p. 307ff.
[50]C. Y. Fong and M. Schlüter in *Electrons and Phonons in Layered Structure,* edited by T. J. Wietring and M. Schlüter (Reidel, Dordrecht, 1986).
[51]V. Grasso and G. Mondio, in *Electronic Structure and Electronic Transitions in Layered Materials,* edited by V. Grasso (Reidel, Dordrecht, 1986).
[52]R. Coehoorn, C. Haas, J. Dijkstra, C. J. F. Flipse, R. A. de Groot, and A. Wold, Phys. Rev. B **35**, 6195 (1987).
[53]W. W. Gärtner, Phys. Rev. **116**, 1 (1959).
[54]J. I. Hanoka and R. O. Bell, Ann. Rev. Mater. Sci. **11**, 353 (1981).
[55]B. Bumüller, diploma thesis, Universität Konstanz (1989).
[56]L. C. Upadhyayula, J. J. Lofersky, A. Wold, W. Giriat, and R. Kershaw, J. Appl. Phys. **39**, 4736 (1968).
[57]C. Clemen, X. I. Saldana, P. Munz, and E. Bucher, Phys. Status Solidi A **49**, 437 (1978).